

1 **Dysregulation of anti-viral function of CD8+T cells in the COPD lung: role of**
2 **the PD1/PDL1 axis¹**

3

4 Richard T. McKendry¹, C. Mirella Spalluto¹, Hannah Burke¹, Ben Nicholas¹,
5 Doriana Cellura¹, Aymen Al-Shamkhani¹, Karl J. Staples^{1*}, Tom MA Wilkinson^{1,2*}.

6 1 University of Southampton Faculty of Medicine, Sir Henry Wellcome
7 Laboratories, Southampton General Hospital, Tremona Road, Southampton,
8 SO16 6YD

9 2 Southampton NIHR Respiratory Biomedical Research Unit, Southampton
10 General Hospital, Tremona Road, Southampton, SO16 6YD

11

12 Running Title: Dysregulation of COPD CD8+ T cells

13 Author contributions: Conception & design – RTM, AAS, KJS & TMAW; Data
14 acquisition, analysis and interpretation – all authors; Drafting of manuscript for
15 important intellectual content – RTM, KJS & TMAW

16 * These authors contributed equally to this work

17 1 This work was part funded by a project grant from Asthma UK (08/026) and the
18 BMA HC Roscoe Award 2013. RTM was funded by a MRC 4-year studentship.

19 2 To whom correspondence should be addressed at: Clinical and Experimental
20 Sciences, University of Southampton Faculty of Medicine, Sir Henry Wellcome
21 Laboratories, Mailpoint 810, Southampton General Hospital, Tremona Road,
22 Southampton, SO16 6YD, UK. Tel: +44 23 8079 6397 Fax: +44 23 8070 1771
23 Email: k.staples@southampton.ac.uk

24 **Running Title: Dysregulation of COPD CD8+ T cells**

25 Manuscript word count: 3499 Abstract word count: 250

26 **At a glance commentary:**

27 **Scientific knowledge on the subject:** Dysregulation of adaptive immunity is
28 thought to be an important disease mechanism in COPD with increased numbers
29 of cytotoxic T cells present in the lung. PD1 is a key regulator of T cell function
30 and is associated with loss of cytotoxic function in the context of chronic infection
31 and inflammation but the role of this axis in COPD and its association with T cell
32 function is not known.

33 **What this study adds to the field:** This study shows that PD1 is upregulated on
34 T cells derived from COPD patients and that PD1 expression increases following
35 influenza infection in an experimental lung explant tissue model. In this study
36 CD8 T cells from COPD patients also demonstrated evidence of impaired
37 cytotoxicity. In contrast, infection-induced expression of the ligand PD-L1 on
38 macrophages was diminished in COPD with associated increases in IFN γ
39 expression. These observations provide evidence of dysregulation of T cell
40 function in COPD through the PD1 axis, contributing to our understanding of
41 mechanisms leading to the aberrant response to infection in COPD.

42 This article has an online data supplement, which is accessible from this issue's
43 table of content online at www.atsjournals.org

44

45 Abstract word count (max 250): 250

46

47 **Abstract**

48 **Rationale:** COPD patients are susceptible to respiratory viral infections which
49 cause exacerbations. Mechanisms underlying susceptibility are not understood.
50 Effectors of the adaptive immune response; CD8+ T cells which clear viral
51 infections, are present in increased numbers in lungs of COPD patients but fail to
52 protect against infection and may contribute to the immunopathology of the
53 disease.

54 **Objectives:** CD8+ function and signalling through the Programmed Cell Death
55 (PD-1) exhaustion pathway was investigated as a potential key mechanism of
56 viral exacerbation of the COPD lung.

57 **Methods:** Tissue from control or COPD patients undergoing lung resection was
58 infected with live influenza virus *ex vivo*. Viral infection and expression of lung
59 cell markers was analysed using flow cytometry.

60 **Measurements and Main Results:** The proportion of lung CD8+ T cells
61 expressing PD-1 was greater in COPD(mean=16.2%) than controls(4.4%,
62 $p=0.029$). Only epithelial cells and macrophages were infected with influenza
63 and there was no difference in the proportion of infected cells between controls
64 and COPD. Infection upregulated T cell PD-1 expression in control and COPD
65 samples. Concurrently, influenza significantly upregulated the marker of
66 cytotoxic degranulation (CD107a) on CD8+ T cells($p=0.03$) from controls, but not
67 from COPD patients. Virus-induced expression of the ligand PD-L1 was
68 decreased on COPD macrophages($p=0.04$) with a corresponding increase in
69 IFN γ release from infected COPD explants compared to controls($p=0.04$).

McKendry page 4

70 **Conclusions:** This study has established a signal of cytotoxic immune
71 dysfunction and aberrant immune regulation in the COPD lung that may explain
72 both the susceptibility to viral infection and the excessive, inflammation
73 associated with exacerbations.

74

75

76 **Introduction**

77 Chronic Obstructive Pulmonary disease (COPD) is an irreversible progressive
78 disease resulting in permanent loss of lung function(1, 2). It is characterised by
79 persistent airflow limitation and innate and adaptive immune cell infiltration into
80 the lungs. COPD patients experience recurrent viral infections accompanied with
81 lung inflammation resulting in exacerbations which are characterised by a
82 sudden decline in lung function, often require hospitalisation, and may result in
83 death(3-5). CD8+ T cells, which play a key role in anti-viral immunity have been
84 shown to be present in greater numbers in the lungs of patients with more severe
85 COPD as measured by FEV₁(6) but these patients remain at great risk from the
86 impacts of respiratory viral infection.

87 Recent studies have suggested that regulation of T cell function can occur
88 via the T cell exhaustion pathway in response to viral infection(7). PD-L1 is the
89 ligand for the Programmed Cell Death protein 1 (PD-1), which is a member of the
90 CD28 family of T cell receptors. The canonical pathway of T cell activation is via
91 antigen presentation in the context of MHC to elicit T cell receptor (TCR)
92 activation, co-stimulation of CD28 provides a necessary signal to prevent T cell
93 anergy(8). Contrastingly, PD-L1 binding to PD-1 causes inhibition of T cell
94 proliferation and cytokine release(9). T cell exhaustion is a state of T cell
95 dysfunction normally associated with chronic viral infection and cancer and is
96 associated with prolonged stimulation of T cells due to persistent antigen
97 presentation. However recent work has suggested that expression of PD-1 is
98 also closely linked to T cell differentiation and can be expressed on acutely

McKendry page 6

99 activated T cells but usually subsides during resolution of infection (10). The PD-
100 1 pathway has recently been suggested as potentially relevant in COPD
101 pathogenesis, as the presence of PD-1+ T effector cells in the blood correlated
102 with disease severity(10). Kalathil *et al.* detected PD-1 expression in a population
103 of blood CD4+CD127+ T cells, although there was no evidence of functional
104 exhaustion(10). The potential for T lymphocytes to express an exhausted
105 phenotype in the COPD lung has not yet been established. We hypothesised that
106 T cells in the COPD lung would express an exhausted phenotype compared to
107 cells derived from control lungs and that T cell exhaustion may account for poor
108 responses to viral infection that may lead to COPD exacerbations.

109

110

111 **Materials & Methods**

112 *Ex vivo infection of lung parenchymal tissue*

113 Resected human lung tissue was obtained from consented patients undergoing
114 airway re-section surgery at our regional thoracic surgical unit. The collection of
115 tissue was approved by and performed in accordance with the ethical standards
116 of the Southampton and South West Hampshire Research Ethics Committee,
117 LREC no: 09/H0504/109. Ex-smokers were defined as individuals who had quit
118 smoking for >6 months. Parenchymal tissue, distant from the resection margin
119 and any gross pathology was dissected from the lobe. Tissue was cut into 1mm³
120 sections and added to a 24-well flat-bottomed culture plate before washing with
121 Dulbecco's Phosphate Buffered Saline (DPBS – Sigma, Poole, UK). Washing of
122 the tissue was performed by removing DPBS from the wells and replacing it with
123 fresh DPBS, followed by unsupplemented RPMI and finally RPMI supplemented
124 with 1% penicillin/streptomycin (both Life Technologies, Paisley, UK) and 1%
125 gentamycin (GE Healthcare, Little Chalfont, UK). Tissue was then incubated
126 overnight at 37°C and 5% CO₂. *Ex vivo* infection of resected lung tissue with
127 H3N2 X31 influenza virus (a kind gift of 3VBiosciences) was then carried out as
128 previously described(11).

129

130 *T cell and Monocyte Isolation & differentiation*

131 CD8+ T cells and Monocytes were isolated from human peripheral blood
132 mononuclear cells (PBMC) using MACS technology (Miltenyi Biotec, Bisley, UK)

133 and monocytes differentiated into macrophages by culturing for 12 days with 2
134 ng/ml GM-CSF.

135

136 *Flow cytometry analysis*

137 Samples were resuspended in FACS buffer (PBS, 0.5% w/v BSA, 2 mM EDTA)
138 containing 200 µg/ml human IgG before being incubated on ice in the dark for 30
139 min in the presence of fluorescently-labelled antibodies as previously
140 described(11). Flow cytometric analysis was performed on a FACSAria using
141 FACSDiva software v5.0.3 (BD Biosciences, Oxford, UK).

142

143 *RNA Isolation & RT-PCR*

144 RNA was extracted from 25,000 flow cytometry sorted CD4+ or CD8+ lung T
145 cells using a Stratagene Nanoprep Kit (Agilent Technologies, Stockport UK).
146 Reverse transcription was carried out using a High Capacity cDNA Reverse
147 Transcription Kit (Life Technologies) with random hexamers carried out
148 according to the manufacturer's protocols. *TIM3* gene expression was analysed
149 using TaqMan universal PCR master mix, No AmpErase® UNG in a 7900HT fast
150 real-time PCR system instrument (all Life Technologies). Gene expression was
151 normalized to β_2 -microglobulin gene expression and quantified using the $\Delta\Delta C_T$
152 method.

153

154 *Supernatant analyses*

155 IFN γ concentrations in culture supernatants were analysed by Luminex assay as
156 per manufacturer's instructions (Bio-Rad, Hemel Hempstead, UK).

157

158 *ELISpot*

159 ELISpot for Human IFN- γ (MabTech, Stockholm, Sweden) was performed using
160 0.45 μ m MultiScreen-IP Filter Plates (Millipore, Watford, UK) as previously
161 described(11). Briefly, MDMs were either not infected, or were treated with 2.5 x
162 10⁴ pfu/ml X31 Influenza A H3N2 virus at 37°C for 2 h before washing and were
163 then added to each well at a concentration of 5 x 10⁴ cells/well and 2.5 x 10⁵
164 monocyte-depleted PBMC or 1 x 10⁵ CD8⁺ T cells were added to MDM-
165 containing wells and incubated at 37°C for a further 22 h.

166

167 *Statistics*

168 Analysis of two groups was performed using Wilcoxon's signed rank test for
169 paired data and a Mann-Whitney U test for unpaired data. Chi-squared test and
170 Fishers exact test were used for categorical data (GraphPad Prism v6, GraphPad
171 Software Inc., San Diego, USA). Results were considered significant if p<0.05.

172

173 For full details of all methods please see supplemental data

174

175 **Results**

176 *Patients*

177 The clinical characteristics of surgical patients are presented in Table 1. COPD
178 patients were matched with controls for age, but had a greater smoking history
179 and lower FEV₁% predicted and greater airflow obstruction.

180

181 *Lung resident T cell phenotype in COPD*

182 Previous studies have demonstrated an increase in CD8+ T cells in the COPD
183 lung by immunohistochemistry (6, 12). To validate our flow cytometry method we
184 measured the proportion of CD4+ and CD8+ T cells disaggregated from the
185 explanted lung tissue using the gating strategy outlined in Figure 1A. The
186 proportion of CD4+ T cells was significantly lower in COPD (mean=39.3%) than
187 controls (mean=47.3%), p=0.016 (Figure 1B). Conversely, the proportion of
188 CD8+ T cells was greater in COPD (mean=42.7%) than controls (31.2%),
189 p=0.004 (Figure 1C & Supplementary Data Figure E1A+B). Moreover the
190 majority of these cells were effector memory cells (CCR7-), suggesting we are
191 studying lung resident cells and not carry over from the blood compartment
192 (Supplementary Data Figure E2).

193

194 *Patients with COPD exhibit elevated proportions of PD1+ T cells*

195 To investigate if the immune defect in CD8+ T cells in COPD was associated with
196 markers of exhaustion, PD-1 expression by lung resident T cells was quantified
197 in control and COPD patients (Figure 2). The mean proportion of CD4+ T cells

198 from controls that expressed PD-1 was 1.68%, compared to a mean of 4.51% in
199 COPD tissue (Figure 2A - $p=0.07$). A mean of 4.39% of CD8+ T cells from control
200 lung tissue expressed PD-1, while a mean of 16.24% expressed PD-1 in COPD
201 tissue (Figure 2B - $p=0.0291$). There was therefore evidence of a greater
202 proportion of T cells expressing PD-1 in COPD lungs compared to control tissue.

203 The co-expression of PD-1 and TIM-3 has been used to identify
204 functionally exhausted T cells in murine models(13). In contrast to PD-1, T cells
205 isolated from tissue of either controls ($n=9$) or COPD individuals ($n=12$) did not
206 express detectable surface TIM-3. To ensure that lack of TIM-3 detection was not
207 due to an effect of collagenase on the lung T cells, RT-PCR experiments were
208 performed using CD4+ and CD8+ T cells sorted from lung parenchyma. TIM-3
209 mRNA was not detected in either CD4+ or CD8+ T cell samples from controls or
210 COPD patients (Supplementary Data Figure E3).

211

212 *Influenza infection of lung explants*

213 In order to assess the functional consequences of a viral infection on the
214 activation of T cells, we utilised a previously validated *ex vivo* model of lung
215 explant infection (11, 14, 15). In that previous study, H3N2 X31 influenza A was
216 shown to infect epithelial cells and macrophages in both human bronchial and
217 parenchymal tissues (11, 15). Endothelium, fibroblasts, B cells and T cells were
218 not infected by X31(14). Therefore infection of epithelial cells and macrophages
219 was quantified using the gating strategy outlined in Figure 3A using the
220 expression of the influenza protein NP-1. Epithelial cells and macrophages from

221 inactivated (UV treated) tissue did not express NP-1. A mean of 10.38% of
222 epithelial cells from control patients expressed NP-1 (Figure 3B) compared to
223 9.19% from COPD samples ($p=0.77$). There were also no significant difference
224 ($p=0.50$) between the proportion of macrophages infected with virus from control
225 (mean 18.12%) or COPD tissue (mean 14.45%) (Figure 3C).

226

227 *T cell responses to influenza infection of lung explants*

228 As there was no difference in the proportion of virally infected cells between
229 healthy and COPD subjects, these data suggest that the mechanisms leading to
230 COPD exacerbations may arise as a failure to adequately control the immune
231 response rather than due to an increased level of infection. PD-1 expression was
232 therefore measured to investigate differential immune responses to infection.
233 Figure 4 shows that PD-1 is upregulated on CD4+ and CD8+ T cells in both
234 control and COPD explants in response to X31 infection (Fig 4A & 4B). CD8+
235 PD-1 expression in controls increased from a mean sMFI of 165.1 to 237.7 in
236 X31 samples ($p=0.01$). *Ex vivo* CD8+ T cells from COPD patients express a
237 mean sMFI PD-1 of 231 which increased to 287.7 with X31 treatment ($p=0.02$). A
238 similar pattern of expression in response to infection was seen for CD4+ T cells.
239 Live virus induced a significantly greater fold increase (median 1.37-fold) in PD-1
240 expression on COPD CD8+ ($p=0.0134$), but not CD4+ ($p=0.2847$), T cells than
241 UV-irradiated virus (Supplementary Data Figure E4C&D). The percentage of
242 CD8+ T cells from both controls and COPD patients expressing PD-1 was also
243 increased in response to X31 treatment. There was also a significant increase in

244 the proportion of CD4⁺ T cell PD-1 expression from COPD patients but not
245 controls in response to infection (Supplementary Data Figure E4A&B). PD-1 is
246 upregulated during X31 infection, but the fold increase in expression induced by
247 influenza in CD4⁺ (p=0.31) and CD8⁺ (p=0.27) T cells did not differ between
248 control and COPD samples (Supplementary Data Figure E4E&F).

249 To analyse the functional relevance of this PD-1 upregulation, we
250 assessed the expression of the degranulation marker CD107a in response to
251 viral infection between controls and COPD individuals (Figure 4C&D). CD4⁺ T
252 cells from both control and COPD samples significantly upregulated CD107a in
253 response to infection (p=0.03) (Figure 4C). In contrast, whilst CD8 T cells from
254 controls significantly upregulated (p=0.03) CD107a in response to viral infection
255 there was not a significant upregulation by CD8 cells derived from COPD
256 explants (Figure 4D). Taken together these results suggest that CD8 T cells in
257 the COPD lung may have an impaired degranulation response to viral infection.

258

259 *Lung macrophage expression of PD-L1 is compromised in COPD*

260 T cells downregulate their effector functions due to ligation of PD-1 by PD-L1. To
261 assess whether there was dysregulation of PD-L1 in our *ex vivo* model, we also
262 measured the expression of this ligand on alveolar epithelial cells and
263 macrophages (Figure 5) and to elucidate whether PD-L1 expression
264 corresponded to viral infection and T cell upregulation of PD-1. The results
265 indicated that epithelial cells express PD-L1 in human parenchyma, but its
266 expression is lower (NI pooled sMFI = 142) than in macrophages (NI pooled

267 sMFI = 442.47) and is not regulated by acute X31 infection (Supplementary Data
268 Figure E5). Macrophages, however, upregulate PD-L1 in response to infection in
269 control samples ($p=0.02$) and COPD samples ($p=0.02$) (Figure 5A). Intriguingly,
270 we observed lower expression of PD-L1 in COPD in response to infection
271 compared to infected control samples ($p = 0.04$) Figure 5B).

272 As PD-L1 has been previously shown to be directly responsible for
273 reducing CD8 T cell function in response to influenza (7), these data suggest that
274 COPD macrophages may be unable to adequately modulate T cell activation. To
275 assess this in the explant model we analysed the release of IFN γ into
276 supernatants from tissue infected with X31 for 24 h (Figure 5C). Infection with
277 influenza caused significant IFN γ release from both control ($p=0.02$) and COPD
278 ($p=0.004$) explants (Figure 5C). However COPD explants produced significantly
279 more IFN γ in response to influenza (mean 86 pg/ml) than infected control
280 explants (mean 49 pg/ml, $p=0.04$) (Figure 5D), suggesting that the decrease in
281 PD-L1 expression by infected macrophages does have a functional effect on T
282 cell cytokine release.

283

284 *Fluticasone does not affect CD8+ T cell PD-1 expression*

285 In order to ensure that the effects we were seeing were not an epiphenomenon
286 due to inhaled corticosteroid use by COPD patients, we incubated peripheral
287 blood derived CD8+ T cells with 10^{-7} M fluticasone propionate (FP) for 24 h and
288 analysed cell surface PD-1 expression by flow cytometry (Figure 6A). There was
289 no significant upregulation of PD-1 on CD8+ T cells in response to fluticasone.

290

291 **Discussion**

292 In the present study, we have demonstrated evidence of dysregulation of T cell
293 immune function in the COPD lung. We have shown that a greater proportion of
294 T cells express PD-1 in COPD tissue than in controls, but that this signal is not
295 one of the canonical fully exhausted phenotype as there was no co-expression of
296 TIM-3 at either the mRNA or protein level. However this finding was associated
297 with evidence of diminished T cell cytotoxic degranulation responses to viral
298 infection. Study of the virus-induced expression of the exhaustion ligand PD-L1
299 demonstrated that it is decreased on COPD macrophages with a corresponding
300 increase in IFN γ release into supernatants from virally infected lung explants.
301 These data are complex to interpret but reflect the complex regulation of T cells
302 in the lung and interactions with the disease effects of COPD. The findings
303 highlight that T cell regulation, of which exhaustion is an important component, is
304 impacted upon by both aberrant T cell functionality and loss of regulatory control
305 in the context of COPD. The consequences of these phenomena may explain the
306 complex relationship between viral susceptibility and excessive inflammation
307 which is the hallmark of acute exacerbations.

308 The increased proportion of CD8 $^{+}$ T cells in the lung parenchyma of
309 COPD patients has been described and it is postulated that this may be due to
310 their anti-viral properties(16, 17). As CD8 $^{+}$ T cells elicit potent anti-viral
311 responses(18), the raised proportions of activated CD8 $^{+}$ T lymphocytes in COPD
312 lungs may indicate a response to increased frequency of infection (19, 20). The
313 localisation of T cells in a murine model of viral infection during RSV or Influenza

314 A virus infection resulted in recruitment of CD8+ T cells to the lungs, with virus
315 specific T cells residing in the lungs for 30 days, with the majority of IFN γ -
316 secreting CD8+ cells being found in lung tissues rather than in the periphery(21).
317 Purwar et al.(22) have shown that human lung contains resident memory T cells
318 (T_{RM}) cells independently of challenge, and these cells can secrete potent
319 inflammatory mediators upon stimulation, underlining the importance of T_{RM} in
320 protecting the host during infection. Recently other work using in vitro stimulation
321 of lung derived T cells has demonstrated evidence of dysfunction in COPD.
322 CD4+ T cells particularly in advanced disease demonstrated aberrant
323 polarization patterns but features of exhaustion or response to direct viral
324 infection were not explored (23).

325 PD-1-expressing lymphocyte populations were identified in lung
326 parenchyma, with a greater proportion of T cells expressing this marker in
327 patients with COPD. This expression was significantly upregulated by CD4+ and
328 CD8+ T cells in response to infection. The inducible nature of PD-1 in response
329 to activation was first identified by Agata *et al.*(24) and this previous work agrees
330 with the findings presented above. PD-1 is a marker of T cell exhaustion, but it is
331 also expressed by activated T cells which appear to be fully or partly functional
332 (25, 26). PD-1 is upregulated by T lymphocytes in acute models of LCMV, but
333 these are resolved before T cells display an exhausted phenotype(27). However,
334 acute infection in the human *ex vivo* model appears to yield similar results to
335 those of the previously reported *in vivo* murine model of influenza infection(28).

336 The release of granzyme B and perforin is utilised by CD8+ T cells to
337 induce apoptosis of virally-infected cells(29). Intracellular staining of these
338 proteins was not performed due to variable levels of Granzyme B detection in
339 unstimulated samples, but CD107a can be used as a surrogate marker for T cell
340 cytotoxic degranulation(29). CD107a was upregulated by CD4 and CD8 T cells in
341 controls but not COPD in response to influenza infection. An inability to produce
342 cytotoxic proteins in response to viral infection infers an associated host
343 susceptibility to infection and potentially a failure to clear the pathogen resulting
344 in prolongation of clinical illness seen in COPD. In combination with the
345 increased PD-1 expression in COPD, these data are consistent with the
346 hierarchical loss of T cell function characteristic of T cell exhaustion(30). These
347 observations suggest that there are an increased proportion of CD8+PD-1+ T
348 cells in the COPD lung that are activated but carry important functional features
349 of exhaustion that have an impaired ability to release cytotoxic granules.

350 Cytotoxic responses are predominantly associated with CD8 T cell and NK
351 cells, but in this model CD107a was also upregulated by CD4 T cells. This finding
352 adds to the growing literature of cytotoxic CD4 T cells in viral infection(31, 32),
353 including influenza(33). It is unclear as to whether cytotoxic CD4+ T cells are a
354 unique subset of T cells, or whether their killing ability is induced during an
355 impaired CD8 response in the context of COPD and this requires further study.

356 Previous investigation into PD-L1 regulation of T cell responses to
357 respiratory viruses has focussed on expression by epithelial cells(7, 34, 35).
358 Influenza viral infection of control and COPD tissue did not modulate PD-L1

359 expression by epithelial cells, even though it was constitutively expressed at a
360 very low level (Supplementary Figure E5). Although there was no difference in
361 the basal expression of this ligand between controls and COPD, macrophages
362 expressed significantly more PD-L1 in response to infection in both groups. Our
363 previous data indicate that this PD-L1 upregulation is functionally relevant, as
364 use of a PD-L1 blocking antibody in our influenza–infected MDM model
365 increased production of IFN γ by autologous CD8 T cells, implicating PD-L1 in the
366 regulation of anti-viral cytokine release(11). In the current study, infected COPD
367 macrophages expressed significantly less PD-L1 than control macrophages,
368 which in turn correlated with an increase in IFN γ release from infected COPD
369 lung. Thus not only does there appear to be a defect in the antiviral cytotoxic
370 function of T cells in COPD but also an inability to arrest the activation of these T
371 cells by decreased PD-L1 expression. These findings are consistent with well
372 recognised clinical phenomena of increased severity of virally infection,
373 prolonged viral shedding and structural lung damage associated with
374 exacerbations.

375 Our previous study suggested that autocrine IFN β production by alveolar
376 macrophages was a driver of PD-L1 expression(11). Rhinovirus-driven asthma
377 exacerbations have been postulated to be a direct result of deficient IFN β
378 production by bronchial epithelial cells from asthmatics for the last decade(36).
379 More recent work challenging COPD patients with rhinovirus to mimic an
380 exacerbation suggests a similar defect in IFN β production may also operate in
381 COPD(37). Unfortunately, we are unable to directly measure IFN β production in

382 virally-challenged lung explants and so deficient production of this cytokine
383 leading to a reduced expression of PD-L1 in response to virus in COPD remains
384 an intriguing possibility.

385 This work has been performed using whole lung explants from patients
386 undergoing thoracic surgery. This approach permits the analysis of the complex
387 interactions between structural and immune cells and the impact of viral infection
388 in this complex composite system. This validated model has contributed to our
389 understanding of cellular immunity in the human lung with a clinically relevant
390 pathogen (live influenza virus) which would be not feasible *in vivo*, but it has
391 limitations when studying immune responses which should be considered. Firstly
392 lung explants are isolated from the effects of immune cells trafficking from the
393 blood and so these conclusions are valid for lung resident cells only. We feel
394 however that, as exhaustion signalling is confined to impacting on terminally
395 differentiated T cells, it remains a very valid model in this context. Furthermore
396 patients donating tissue were undergoing surgery for indications including lung
397 cancer which may impact on the findings. However only tissue distant to the
398 tumour site was used and the COPD related effects on immunity were apparent
399 whilst the co-morbidities leading to surgery were present in both COPD and
400 controls. In using lung derived T cells we have been limited in the number of cells
401 available for phenotypic analysis and hence the breadth of phenotypic markers
402 was also constrained to a single flow cytometry panel. We have used established
403 markers to identify T cells and their function. Cytotoxic function can be measured
404 in a number of ways including expression of perforin and granzyme B as well as

405 the marker CD107a. This latter marker has been well established as a signature
406 of cytotoxic degranulation(7, 38). However to fully understand the dysfunctional
407 nature of T cells further studies exploring functional killing ability and the antigen
408 specific nature of dysfunctional T cell subsets are required. In addition the
409 interaction with functional readouts of T cells and the response to infection with
410 treatments such as inhaled corticosteroids and also active smoking requires
411 further study to provide insights into how these may diminish protective immunity.

412 Taken together, these data indicate a dysregulation of CD8+ T cell
413 responses to viral infection in the COPD lung. Moreover, they suggest that viral
414 exacerbations of COPD may arise due to a combination of an already active CD8
415 T cell population with an impaired anti-viral action coupled with an inability to
416 down-regulate cytokine release from these as a result of deficient PD-L1
417 expression. However interpretation of the observed results requires caution as it
418 is possible that reduction of PD-L1 expression enables increased IFN γ
419 expression which aids viral clearance in the diseased lung. Whichever the
420 direction of effect *in vivo*, these observations have important potential
421 implications for the therapeutic manipulation of T cell function including the use of
422 PD-1 and PD-L1 blocking antibodies to modulate T cell activity which are in use
423 as cancer therapies today. Further studies are required to investigate the
424 translational potential of this approach. If this axis is modulated imprecisely, risks
425 to the patient of pneumonitis, are already recognised(39). The key question
426 remains as to what drives the increased expression of PD-1 in the COPD airway

427 and whether cells manifesting this functional phenotype are the ones specific to
428 pathogens or autoantigens that play a key role in the pathogenesis of COPD.
429

430

	Control	COPD	p Value
N	24	33	-
Age (years)	70.5 (61 – 76)	67 (60.5 – 74)	0.75#
Gender M/F	12 / 12	16 / 17	0.91†
BMI	27.25 (22.63 – 31.55)	23.7 (21.25 – 28.95)	0.23#
Confirmed corticosteroid use	1	9	0.0336‡
Smoker (Never/Ex/Current)	6 / 15 / 3	1 / 20 / 12	0.0671‡
Pack Years	21 (.625 – 52.5)	40 (31.25 – 62.5)	0.025#
FEV ₁ %	98 (91.9 – 112)	76.13 (67 – 86)	< 0.0001#
FEV ₁ /FVC ratio	0.776 (0.73 – 0.805)	0.601 (0.551 – 0.654)	< 0.0001#

431 **Table 1: Clinical characteristics of surgical patients.** Data are presented as
 432 median and IQR shown. Ex-smokers were defined as individuals who had
 433 stopped smoking for > 6 months prior to surgery. BMI data shown represents 16
 434 Control and 17 COPD patients. #Mann Whitney U Test, †Chi-squared test, ‡
 435 Fishers Exact test. Co-morbidity data can be viewed in Supplementary Table E3.

436

437

438

439 **Acknowledgements**

440 The authors wish to thank Richard Jewell and Dr Carolann MacGuire of the
441 University of Southampton Faculty of Medicine Flow Cytometry Unit. We would
442 also like to express our appreciation to the Director Professor Ratko Djukanovic
443 and staff of the Southampton NIHR Respiratory Biomedical Research Unit and
444 the Southampton Cardiothoracic Surgical team led by Mr Aiman Alzetani. The
445 assistance of Dr. Ngaire Coombs was greatly appreciated for ensuring
446 appropriate statistical tests were performed. Furthermore we wish to express our
447 gratitude to Dr. Jane Warner and colleagues who assisted in acquisition of
448 human lung tissue. We extend our gratitude to all the volunteers who gave of
449 their time and enthusiasm to make this research possible.

450

451 **References**

452

453 1. Fletcher C, Peto R. The natural history of chronic airflow obstruction. *Br Med J*

454 1977; 1: 1645-1648.

455 2. GOLD. Global Strategy for the Diagnosis, Management and Prevention of

456 COPD. 2014.

457 3. Chapman KR, Mannino DM, Soriano JB, Vermeire PA, Buist AS, Thun MJ,

458 Connell C, Jemal A, Lee TA, Miravittles M, Aldington S, Beasley R.

459 Epidemiology and costs of chronic obstructive pulmonary disease. *Eur*460 *Respir J* 2006; 27: 188-207.

461 4. Hilleman DE, Dewan N, Malesker M, Friedman M. Pharmacoeconomic

462 evaluation of COPD. *Chest* 2000; 118: 1278-1285.463 5. Sullivan SD, Ramsey SD, Lee TA. The economic burden of COPD. *Chest*

464 2000; 117: 5S-9S.

465 6. O'Shaughnessy TC, Ansari TW, Barnes NC, Jeffery PK. Inflammation in

466 bronchial biopsies of subjects with chronic bronchitis: inverse relationship

467 of CD8+ T lymphocytes with FEV1. *Am J Respir Crit Care Med* 1997; 155:

468 852-857.

469 7. Erickson JJ, Gilchuk P, Hastings AK, Tollefson SJ, Johnson M, Downing MB,

470 Boyd KL, Johnson JE, Kim AS, Joyce S, Williams JV. Viral acute lower

471 respiratory infections impair CD8+ T cells through PD-1. *J Clin Invest*

472 2012.

- 473 8. Schwartz RH. Costimulation of T lymphocytes: the role of CD28, CTLA-4, and
474 B7/BB1 in interleukin-2 production and immunotherapy. *Cell* 1992; 71:
475 1065-1068.
- 476 9. Keir ME, Francisco LM, Sharpe AH. PD-1 and its ligands in T-cell immunity.
477 *Current opinion in immunology* 2007; 19: 309-314.
- 478 10. Kalathil SG, Lugade AA, Pradhan V, Miller A, Parameswaran GI, Sethi S,
479 Thanavala Y. T-regulatory cells and programmed death 1(+) T cells
480 contribute to effector T-cell dysfunction in patients with chronic obstructive
481 pulmonary disease. *Am J Respir Crit Care Med* 2014; 190: 40-50.
- 482 11. Staples KJ, Nicholas B, McKendry RT, Spalluto CM, Wallington JC, Bragg
483 CW, Robinson EC, Martin K, Djukanovic R, Wilkinson TM. Viral infection
484 of human lung macrophages increases PDL1 expression via IFNbeta.
485 *PloS one* 2015; 10: e0121527.
- 486 12. Saetta M, Di Stefano A, Turato G, Facchini FM, Corbino L, Mapp CE,
487 Maestrelli P, Ciaccia A, Fabbri LM. CD8+ T-lymphocytes in peripheral
488 airways of smokers with chronic obstructive pulmonary disease. *Am J*
489 *Respir Crit Care Med* 1998; 157: 822-826.
- 490 13. Jin HT, Anderson AC, Tan WG, West EE, Ha SJ, Araki K, Freeman GJ,
491 Kuchroo VK, Ahmed R. Cooperation of Tim-3 and PD-1 in CD8 T-cell
492 exhaustion during chronic viral infection. *Proc Natl Acad Sci U S A* 2010;
493 107: 14733-14738.

McKendry page 26

- 494 14. Nicholas B, Staples K, Moese S, Ward J, North M, Wilkinson T, Pink S,
495 Djukanovic R. Validation Of Anti-Host Cell Influenza Targets Using A
496 Novel Human Lung Tissue Model. *American journal of respiratory and*
497 *critical care medicine* 2012; 185: A5716.
- 498 15. Nicholas B, Staples KJ, Moese S, Meldrum E, Ward J, Dennison P, Havelock
499 T, Hinks TS, Amer K, Woo E, Chamberlain M, Singh N, North M, Pink S,
500 Wilkinson TM, Djukanovic R. A novel lung explant model for the ex vivo
501 study of efficacy and mechanisms of anti-influenza drugs. *Journal of*
502 *Immunology* 2015; 194: 6144-6154.
- 503 16. Yap KL, Ada GL, McKenzie IF. Transfer of specific cytotoxic T lymphocytes
504 protects mice inoculated with influenza virus. *Nature* 1978; 273: 238-239.
- 505 17. Topham DJ, Tripp RA, Doherty PC. CD8+ T cells clear influenza virus by
506 perforin or Fas-dependent processes. *Journal of immunology* 1997; 159:
507 5197-5200.
- 508 18. Mueller SN, Langley WA, Carnero E, Garcia-Sastre A, Ahmed R.
509 Immunization with live attenuated influenza viruses that express altered
510 NS1 proteins results in potent and protective memory CD8+ T-cell
511 responses. *Journal of virology* 2010; 84: 1847-1855.
- 512 19. Benfield T, Lange P, Vestbo J. COPD stage and risk of hospitalization for
513 infectious disease. *Chest* 2008; 134: 46-53.

- 514 20. Sethi S, Evans N, Grant BJ, Murphy TF. New strains of bacteria and
515 exacerbations of chronic obstructive pulmonary disease. *N Engl J Med*
516 2002; 347: 465-471.
- 517 21. Knudson CJ, Weiss KA, Hartwig SM, Varga SM. The pulmonary localization
518 of virus-specific T lymphocytes is governed by the tissue tropism of
519 infection. *J Virol* 2014; 88: 9010-9016.
- 520 22. Purwar R, Campbell J, Murphy G, Richards WG, Clark RA, Kupper TS.
521 Resident memory T cells (T(RM)) are abundant in human lung: diversity,
522 function, and antigen specificity. *PloS one* 2011; 6: e16245.
- 523 23. Freeman CM, McCubbrey AL, Crudgington S, Nelson J, Martinez FJ, Han
524 MK, Washko GR, Jr., Chensue SW, Arenberg DA, Meldrum CA,
525 McCloskey L, Curtis JL. Basal gene expression by lung CD4+ T cells in
526 chronic obstructive pulmonary disease identifies independent molecular
527 correlates of airflow obstruction and emphysema extent. *PloS one* 2014;
528 9: e96421.
- 529 24. Agata Y, Kawasaki A, Nishimura H, Ishida Y, Tsubata T, Yagita H, Honjo T.
530 Expression of the PD-1 antigen on the surface of stimulated mouse T and
531 B lymphocytes. *Int Immunol* 1996; 8: 765-772.
- 532 25. Wu X, Zhang H, Xing Q, Cui J, Li J, Li Y, Tan Y, Wang S. PD-1(+) CD8(+) T
533 cells are exhausted in tumours and functional in draining lymph nodes of
534 colorectal cancer patients. *British journal of cancer* 2014; 111: 1391-1399.

- 535 26. Utzschneider DT, Legat A, Fuertes Marraco SA, Carrie L, Luescher I, Speiser
536 DE, Zehn D. T cells maintain an exhausted phenotype after antigen
537 withdrawal and population reexpansion. *Nat Immunol* 2013.
- 538 27. Barber DL, Wherry EJ, Masopust D, Zhu B, Allison JP, Sharpe AH, Freeman
539 GJ, Ahmed R. Restoring function in exhausted CD8 T cells during chronic
540 viral infection. *Nature* 2006; 439: 682-687.
- 541 28. McNally B, Ye F, Willette M, Flano E. Local Blockade of Epithelial PDL-1 in
542 the Airways Enhances T Cell Function and Viral Clearance during
543 Influenza Virus Infection. *J Virol* 2013; 87: 12916-12924.
- 544 29. Peters PJ, Borst J, Oorschot V, Fukuda M, Krahenbuhl O, Tschopp J, Slot
545 JW, Geuze HJ. Cytotoxic T lymphocyte granules are secretory lysosomes,
546 containing both perforin and granzymes. *J Exp Med* 1991; 173: 1099-
547 1109.
- 548 30. Wherry EJ. T cell exhaustion. *Nat Immunol* 2011; 12: 492-499.
- 549 31. Fang M, Siciliano NA, Hersperger AR, Roscoe F, Hu A, Ma X, Shamsedeen
550 AR, Eisenlohr LC, Sigal LJ. Perforin-dependent CD4+ T-cell cytotoxicity
551 contributes to control a murine poxvirus infection. *Proc Natl Acad Sci U S*
552 *A* 2012.
- 553 32. Jellison ER, Kim SK, Welsh RM. Cutting edge: MHC class II-restricted killing
554 in vivo during viral infection. *Journal of immunology* 2005; 174: 614-618.

- 555 33. Wilkinson TM, Li CK, Chui CS, Huang AK, Perkins M, Liebner JC, Lambkin-
556 Williams R, Gilbert A, Oxford J, Nicholas B, Staples KJ, Dong T, Douek
557 DC, McMichael AJ, Xu XN. Preexisting influenza-specific CD4(+) T cells
558 correlate with disease protection against influenza challenge in humans.
559 *Nat Med* 2012.
- 560 34. Stanciu LA, Bellettato CM, Laza-Stanca V, Coyle AJ, Papi A, Johnston SL.
561 Expression of programmed death-1 ligand (PD-L) 1, PD-L2, B7-H3, and
562 inducible costimulator ligand on human respiratory tract epithelial cells and
563 regulation by respiratory syncytial virus and type 1 and 2 cytokines. *The*
564 *Journal of infectious diseases* 2006; 193: 404-412.
- 565 35. Telcian AG, Laza-Stanca V, Edwards MR, Harker JA, Wang H, Bartlett NW,
566 Mallia P, Zdrenghea MT, Keadze T, Coyle AJ, Openshaw PJ, Stanciu
567 LA, Johnston SL. RSV-induced bronchial epithelial cell PD-L1 expression
568 inhibits CD8+ T cell nonspecific antiviral activity. *The Journal of infectious*
569 *diseases* 2011; 203: 85-94.
- 570 36. Wark PA, Johnston SL, Bucchieri F, Powell R, Puddicombe S, Laza-Stanca
571 V, Holgate ST, Davies DE. Asthmatic bronchial epithelial cells have a
572 deficient innate immune response to infection with rhinovirus. *The Journal*
573 *of experimental medicine* 2005; 201: 937-947.
- 574 37. Mallia P, Message SD, Gielen V, Contoli M, Gray K, Keadze T, Aniscenko J,
575 Laza-Stanca V, Edwards MR, Slater L, Papi A, Stanciu LA, Kon OM,
576 Johnson M, Johnston SL. Experimental rhinovirus infection as a human

577 model of chronic obstructive pulmonary disease exacerbation. *Am J*
578 *Respir Crit Care Med* 2011; 183: 734-742.

579 38. Betts MR, Brenchley JM, Price DA, De Rosa SC, Douek DC, Roederer M,
580 Koup RA. Sensitive and viable identification of antigen-specific CD8+ T
581 cells by a flow cytometric assay for degranulation. *J Immunol Methods*
582 2003; 281: 65-78.

583 39. Topalian SL, Hodi FS, Brahmer JR, Gettinger SN, Smith DC, McDermott DF,
584 Powderly JD, Carvajal RD, Sosman JA, Atkins MB, Leming PD, Spigel
585 DR, Antonia SJ, Horn L, Drake CG, Pardoll DM, Chen L, Sharfman WH,
586 Anders RA, Taube JM, McMiller TL, Xu H, Korman AJ, Jure-Kunkel M,
587 Agrawal S, McDonald D, Kollia GD, Gupta A, Wigginton JM, Sznol M.
588 Safety, Activity, and Immune Correlates of Anti-PD-1 Antibody in Cancer.
589 *N Engl J Med* 2012.

590
591

592 **Figure Legends**

593

594 **Figure 1. Flow cytometry gating strategy for T cells in lung parenchymal**
595 **tissue.** After resting explanted lung tissue overnight, tissue was digested with
596 collagenase and cells analysed by flow cytometry **(A)** Unstained singlet
597 population was obtained from digested tissue. Dead cells were excluded using
598 LIVE/DEAD® Fixable Aqua Dead Cell Stain. Live singlet CD45+ population was
599 then identified and from this a CD45+CD3+ T cell population. The CD45+CD3+ T
600 cell population was divided into CD4+ and CD8+ T cells. **(A)** Proportion of CD4+
601 **(B)** and CD8+ T cells are gated on the live CD45+CD3+ population. Control n =
602 20, COPD n = 24. Median and IQR shown. Data analysed using a Mann-Whitney
603 U-test # p<0.05, ## p<0.01.

604

605 **Figure 2. Intrinsic PD-1 expression by CD4 and CD8 T cells in controls and**
606 **COPD.** After resting explanted lung tissue overnight, tissue was digested with
607 collagenase and cells analysed by flow cytometry. T cells are gated on the live
608 CD45+CD3+ population. **(A)** Proportion of CD4+ **(B)** and CD8+ T cells
609 expressing surface PD-1. Control n = 9, COPD n = 12. Median and IQR shown.
610 Data analysed using a Mann-Whitney U-test # p<0.05. Note that y axis limit is
611 changed from 15% to 50% between **(A)** and **(B)**.

612

613 **Figure 3. Infection of Epithelial cells and Macrophages from lung**
614 **parenchymal tissue.** After resting explanted lung tissue overnight, 1×10^6 pfu/ml

McKendry page 32

615 H3N2 X31 influenza virus or a UV-irradiated aliquot of virus (UVX31) was added
616 for 2 h. After washing, media was replaced and the tissue was incubated for a
617 further 22 h followed by collagenase digestion and flow cytometry analysis **(A)**
618 Epithelial cells were identified as CD45- EpCAM+ cells. Macrophages were
619 identified as CD45+ HLA-DR+ cells. **(B)** Proportion of Epithelial cells and **(C)**
620 Macrophages expressing NP-1 after treatment with 1×10^6 pfu/ml live X31 virus
621 (X31), UV-irradiated virus (UVX31) or non-infected (NI). NP-1+ cells were
622 classified as infected by the influenza virus. Median and IQR shown. Data
623 analysed using Wilcoxon's signed rank test (** $p < 0.01$, *** $p < 0.001$) to analyse
624 intra group variations and Mann-Whitney U-test to analyse intergroup variations.
625 (n.s. = not significant)

626

627 **Figure 4. Expression of PD-1 and CD107a by T cells in response to tissue**
628 **infection by X31 influenza. (A)** CD4+ **(B)** and CD8+ T cell expression of PD-1
629 was quantified by flow cytometry in non-infected (NI), live X31 virus infection
630 (X31) and UV-irradiated virus (UVX31) lung samples. Control n = 9, COPD n =
631 12. **(C)** CD4+ **(D)** and CD8+ T cells expression of CD107a was also quantified by
632 flow cytometry. Control n = 6, COPD n = 6. Median and IQR shown. Data
633 analysed using a Wilcoxon-signed rank test (* $p < 0.05$, ** $p < 0.01$) and Mann-
634 Whitney U-test to analyse intergroup variations.

635

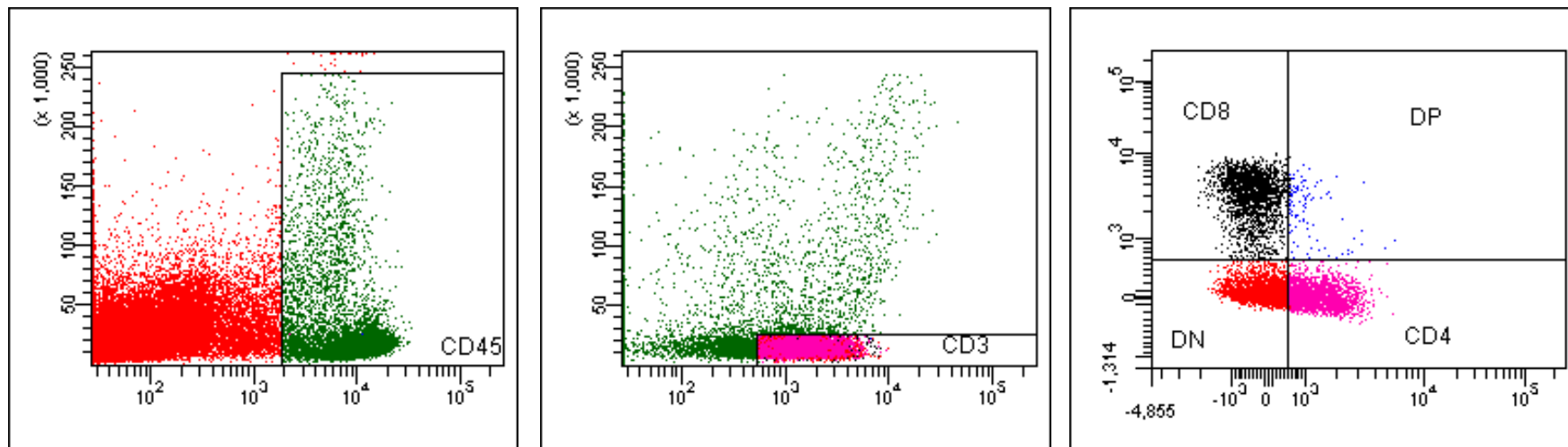
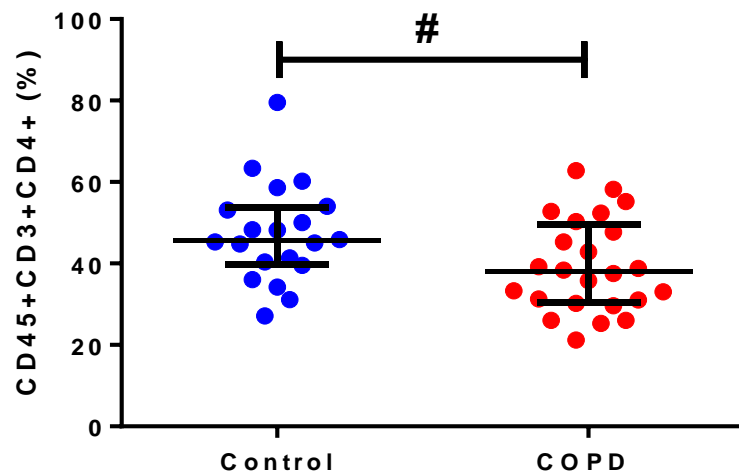
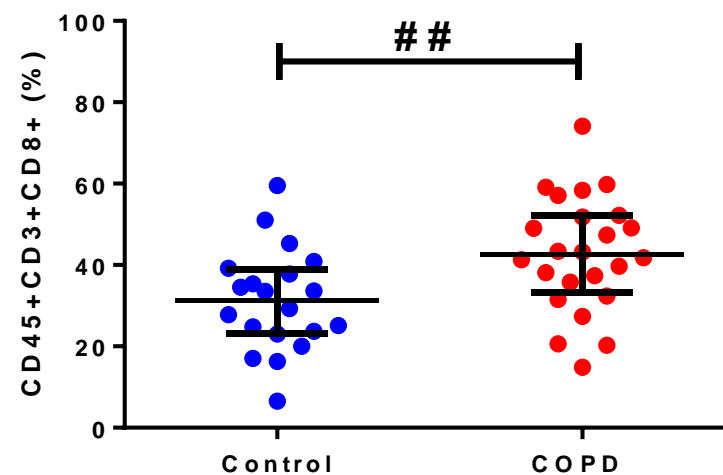
636 **Figure 5. Expression of PD-L1 by Macrophages and IFN γ production in**
637 **response to tissue infection by X31 influenza. (A)** Expression of PD-L1 by

638 Macrophages was measured in non-infected (NI), live X31 virus infection (X31)
639 and UV-irradiated virus (UVX31) samples. **(B)** Differences in PD-L1 expression
640 between X31 control and X31 COPD samples. Control n = 9, COPD n = 11. **(C)**
641 IFN γ was measured from supernatants of non-infected (NI), live X31 virus
642 infection (X31) and UV-irradiated virus (UVX31) explant tissue. **(D)** Differences in
643 IFN γ production between X31 control and X31 COPD samples. Control n = 10,
644 COPD n = 8. Median and IQR are shown. Data in (A) & (C) were analysed using
645 a Wilcoxon-signed rank test_* p<0.05, ** p<0.01. Data in (B) & (D) were analysed
646 using a Mann-Whitney U test # p<0.05, ## p<0.01.

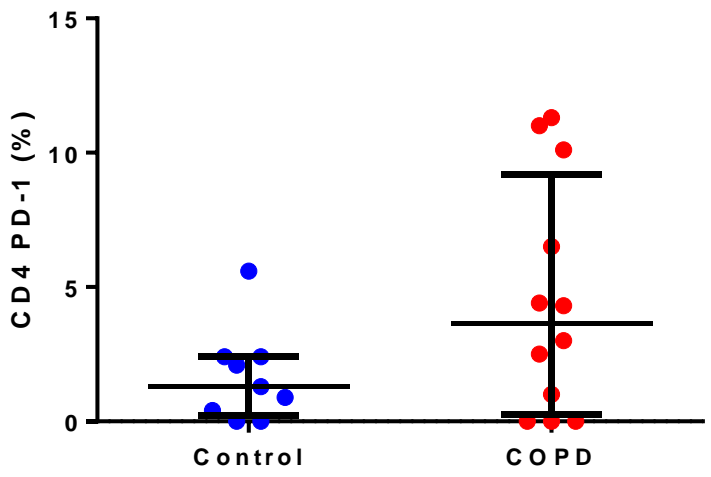
647

648 **Figure 6. Effect of Fluticasone Propionate on blood CD8+ T cell PD1**
649 **expression** PD-1 expression was measured in non-infected blood CD8 T cells
650 incubated in the presence or absence of 10⁻⁷M FP by flow cytometry (n=4).
651 Median and IQR are shown. Data were analysed using a Wilcoxon-signed rank
652 test.

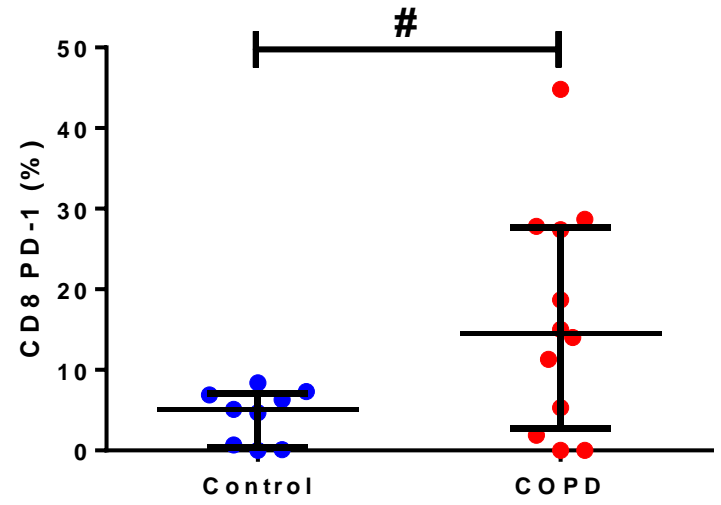
653

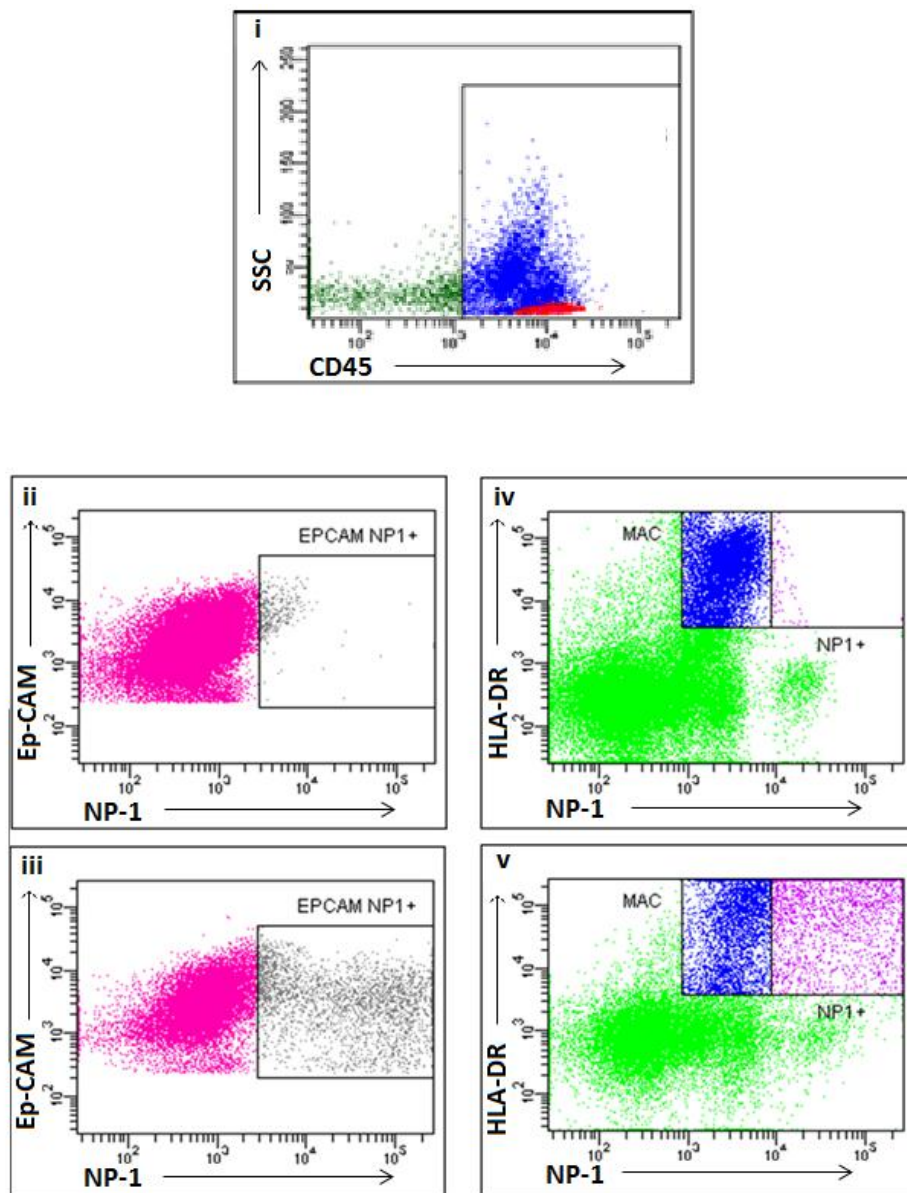
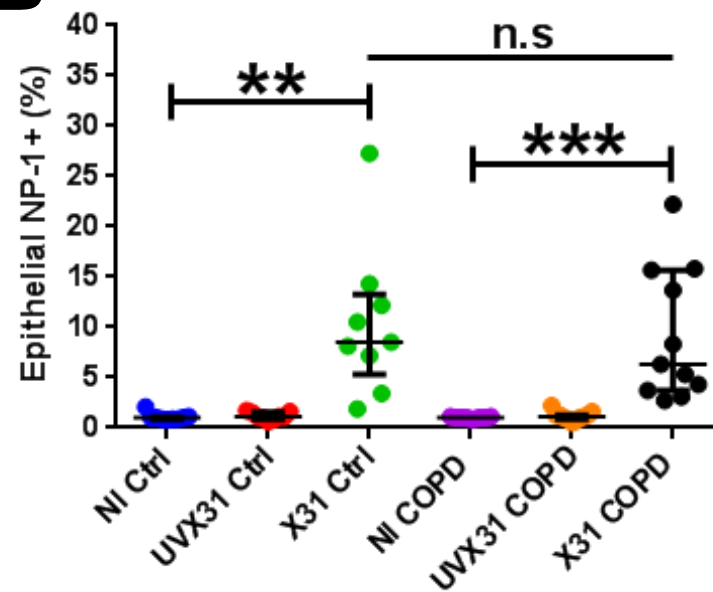
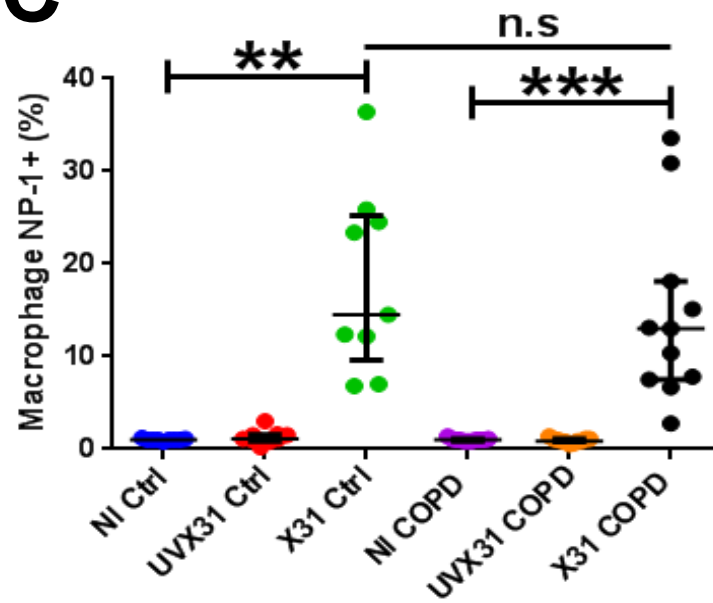
A**B****C**

A

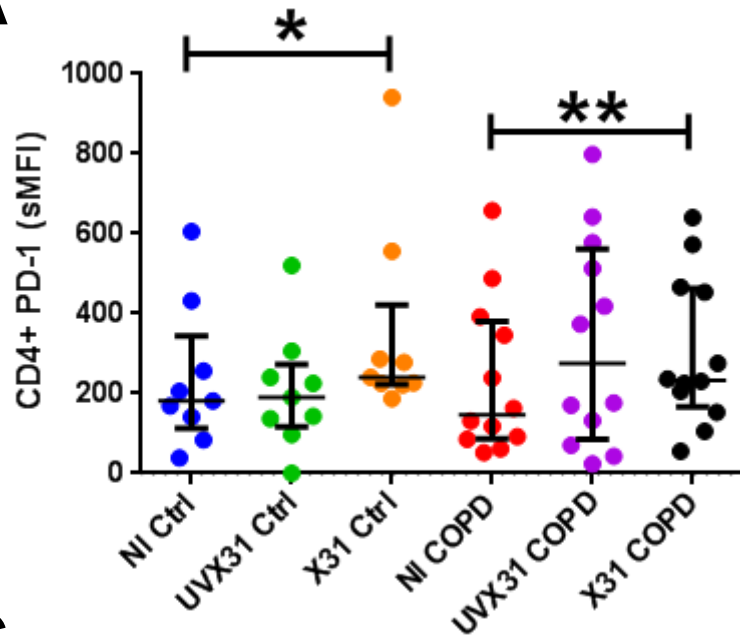


B

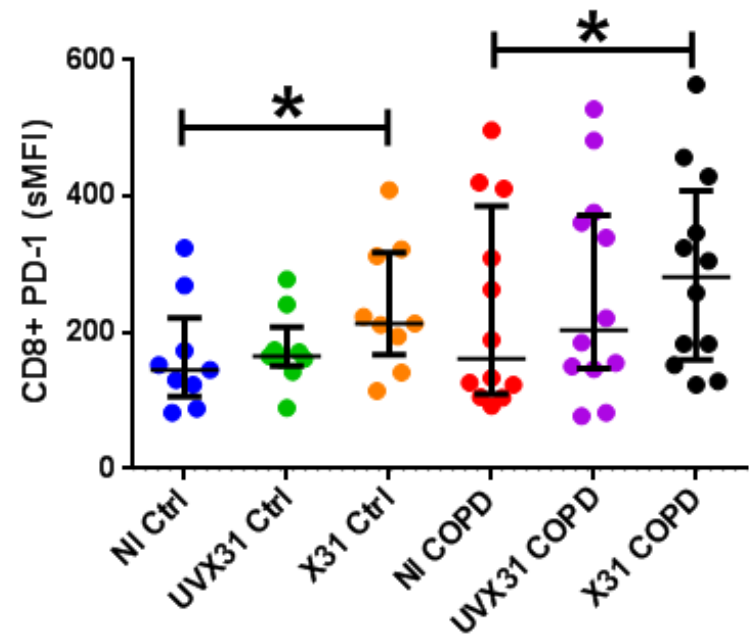


A**B****C**

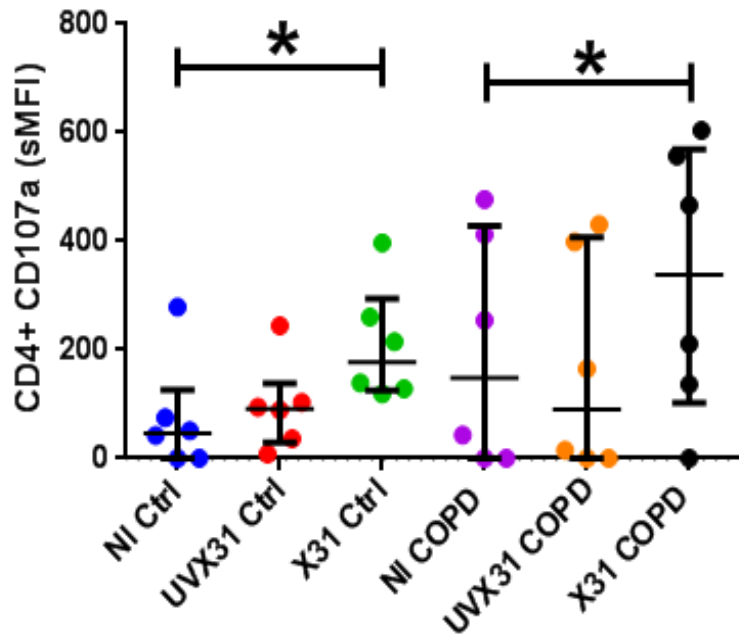
A



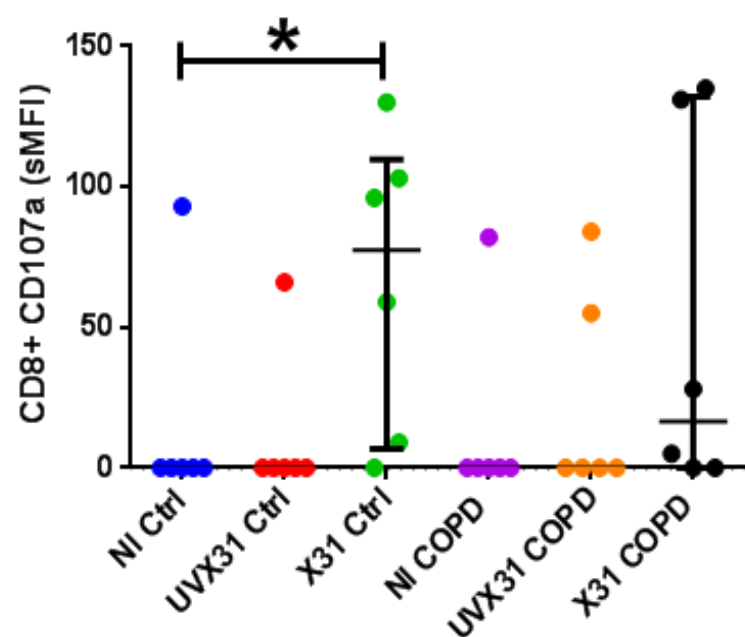
B

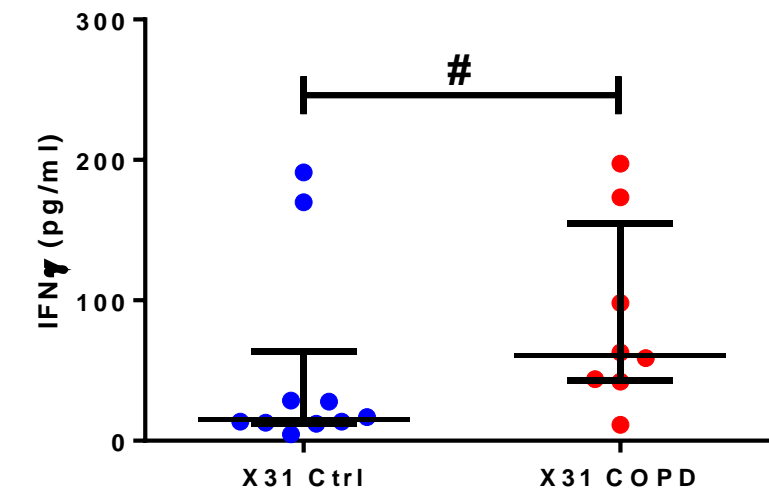
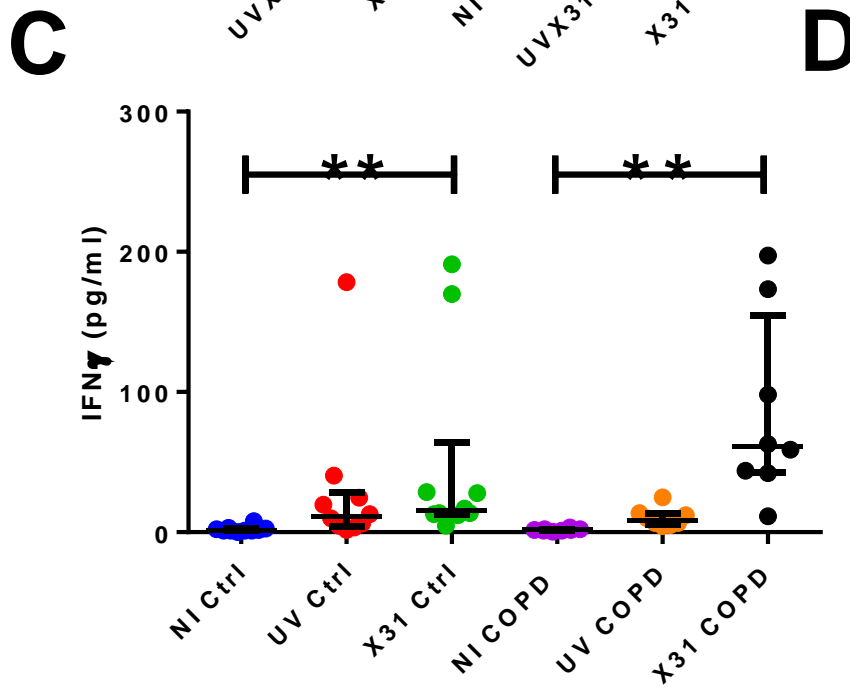
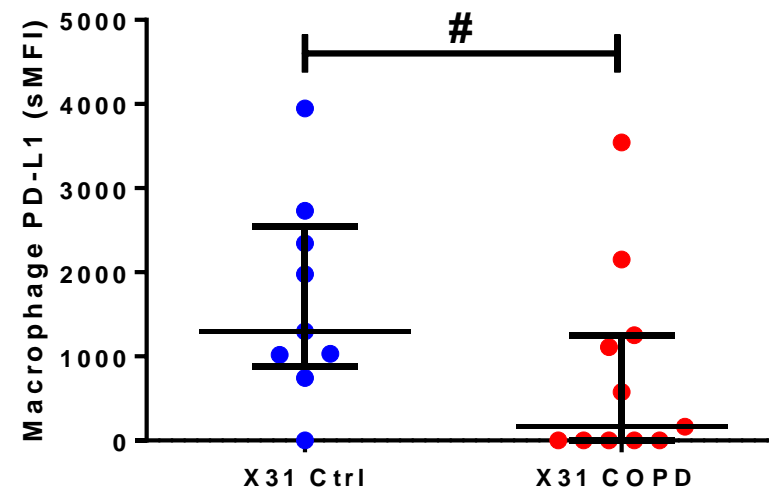
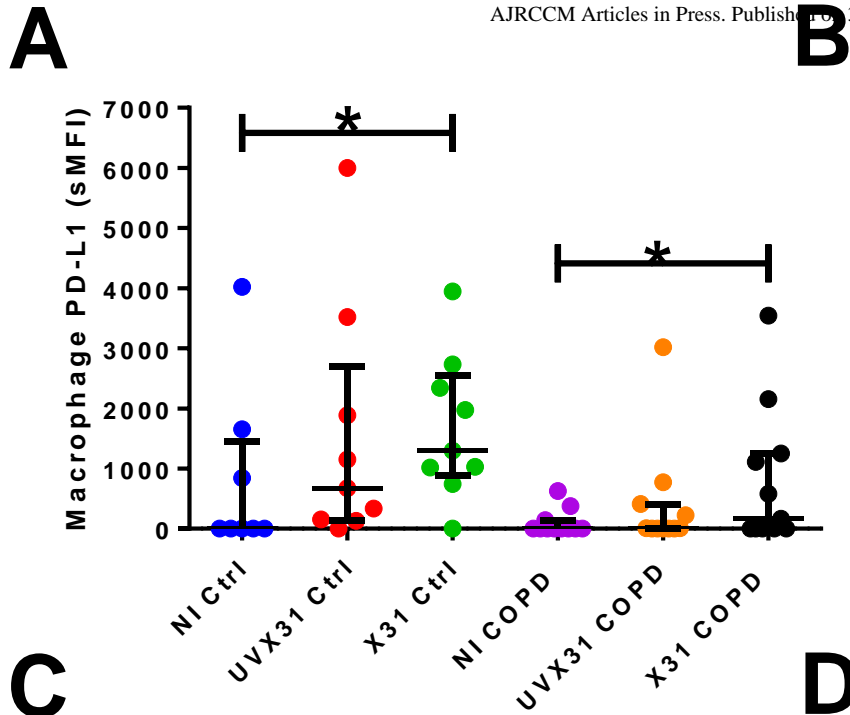


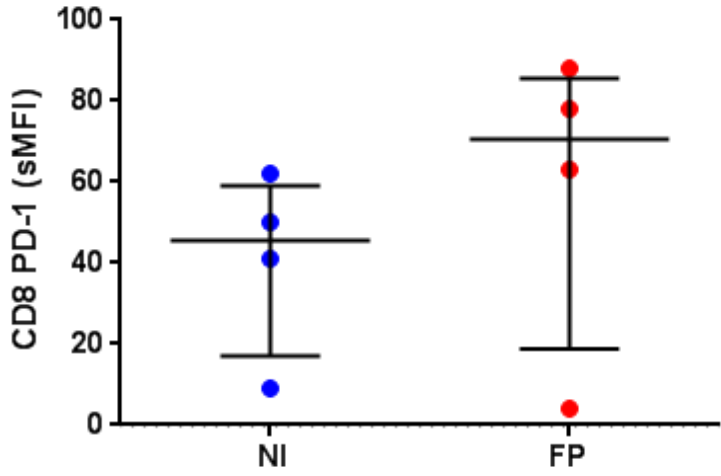
C



D







1 **Online supplement for:**

2

3 **Dysregulation of anti-viral function of CD8+T cells in the COPD lung: role of**
4 **the PD1/PDL1 axis**

5

6 Richard T. McKendry, C. Mirella Spalluto, Hannah Burke, Ben Nicholas, Doriana

7 Cellura, Aymen Al-Shamkhani, Karl J. Staples, Tom M A Wilkinson.

8

9 **Methods**

10 ***Ex vivo* infection of resected human lung tissue**

11 Lung tissue was obtained from patients undergoing airway re-sectioning surgery at
12 Southampton General Hospital. The collection of tissues was approved by and
13 performed in accordance with the ethical standards of the Southampton and South
14 West Hampshire Research Ethics Committee, LREC no: 09/H0504/109.
15 Parenchymal tissue, distant from the resection margin and any gross pathology was
16 dissected from the lobe. Tissue was cut into 1mm³ sections and added to a 24-well
17 flat-bottomed culture plate before washing with DPBS (Sigma, Poole, UK). Washing
18 of the tissue was performed by removing DPBS from the wells and replacing it with
19 fresh DPBS, followed by unsupplemented RPMI and finally RPMI supplemented with
20 1% penicillin/streptomycin ((both Life Technologies, Paisley, UK) and 1%
21 gentamycin (GE Healthcare, Little Chalfont, UK). Tissue was then incubated
22 overnight at 37°C and 5% CO₂.

23 Tissue was infected and analysed according to according to the method
24 described by Staples et al(1). After resting overnight the media was replaced with
25 serum-free RPMI supplemented with 100 U/ml penicillin, 100 µg/ml streptomycin, 2
26 mM L-glutamine and 250 ng/ml fungizone. Influenza A virus strain X31 was supplied
27 at a concentration of 4 x 10⁷ pfu/ml (a kind gift of 3VBiosciences). Inactivated virus
28 (UVX31) was prepared by exposure of the X31 to an ultra-violet (UV) light source for
29 2 h. X31 or UVX31 at a concentration of 1 x 10⁶ pfu/ml was added to designated
30 wells, with control non-infected wells. Tissue was incubated at 37°C and 5% CO₂ for
31 2 h to allow for infection of cells residing in the tissue. Supernatant was removed and
32 tissue was washed three times with unsupplemented RPMI in order to remove
33 excess virus from the wells. Serum-free RPMI supplemented with 100 U/ml penicillin,

34 100 µg/ml streptomycin, 2 mM L-glutamine and 250 ng/ml fungizone was added to
35 the wells and tissue was incubated at 37°C and 5% CO₂ for a further 22 h.

36 Protocol used to digest tissue was adapted from Holt *et al* (2). Briefly, Tissue
37 was added to a solution of pre-warmed unsupplemented RPMI and 0.5 mg/ml
38 collagenase type I (Sigma) for digestion. A magnetic stirrer was added to the solution
39 in order to mechanically disaggregate tissue. Collagenase digestion occurred at
40 37°C for 15 min. This tissue digestion protocol was optimised using blood-derived
41 cells to ensure there was no effect on the major T cell markers expressed on naive
42 blood cells. After digestion the solution was filtered through a 35 µm pore straining
43 cap into 5 ml round-bottomed polypropylene FACS tubes (BD Biosciences) in
44 preparation for FACS analysis.

45

46 **Monocyte Isolation & differentiation**

47 Human peripheral blood mononuclear cells (PBMC) were isolated from heparinised
48 blood by centrifugation on Ficoll-Paque® (GE Healthcare, Little Chalfont, UK).
49 Monocytes were then isolated from the PBMC using CD14+ microbeads (Miltenyi-
50 Biotec, Bisley, UK) according to the manufacturer's instructions. Isolated monocytes
51 were resuspended in complete RPMI supplemented with 2 ng/ml GM-CSF (R&D
52 Systems, Abingdon, UK). MDM were then washed extensively with basal RPMI
53 before addition of virus RS-RPMI. Collection of samples for this part of the study
54 was approved by the Southampton and South West Hampshire Research Ethics
55 Committee (reference: 08/H0504/138). CD8+ T cells were isolated from the
56 monocyte-depleted PBMC that resulted from this separation step using CD8+
57 microbeads (Miltenyi-Biotec) before freezing at -80°C in 10% (v/v) DMSO/HI-FBS for
58 use in later ELISpot analysis.

59

60 Infection of lung macrophages and MDM

61 Influenza A virus strain X31 was supplied at a concentration of 4×10^7 pfu/ml (a kind
62 gift of 3VBiosciences). Inactivated virus (UVX31) was prepared by exposure of the
63 X31 to an ultra-violet (UV) light source for 2 h. Macrophages were incubated for 2 h
64 with no virus, or 4000 pfu (lung) or 500 pfu (MDM) of X31 or UVX31. Supernatants
65 were harvested (T-2), the cells washed three times, the final wash was harvested
66 (T0) and fresh RS media was added to the MDMs. Cells were then washed and
67 incubated for a further 22 h at 37°C, 5% CO₂. After a further 22 h, supernatants were
68 harvested (T22) for cytokine analysis and cells collected and immediately analysed
69 by flow cytometry. For phenotypic characterisation of influenza infected
70 macrophages, cells were removed from culture plates using a non-enzymatic cell
71 dissociation solution (Sigma).

72

73 Flow cytometry analysis

74 Samples were resuspended in FACS buffer (PBS, 0.5% w/v BSA, 2 mM EDTA)
75 containing 200 µg/ml human IgG (Sigma).

76 Lung explants:

77 Single cell suspensions derived from collagenase digestion were incubated on ice in
78 the dark for 30 min with the following antibodies: Phycoerythrin-CF594 (PE-CF-594)-
79 conjugated anti-CD45, Peridinin-Chlorophyll Protein-Cyanine 5.5 (PerCPCy-5.5)-
80 conjugated anti-EpCAM-1 (CD326), and Allophycocyanin-Cyanine 7 (APC-Cy7)-
81 conjugated anti-HLA-DR, Phycoerythrin (PE)-conjugated anti-PD-L1, PE-Cy7
82 conjugated anti-CD3, PerCPCy5.5-conjugated anti-CD4 and APC-Cy7-conjugated
83 anti-CD8 (All BD Biosciences, Oxford, UK). Appropriate isotype and fluorescence-

84 matched control antibodies were added in a sample of the cells to aid gating of cell
85 populations. After washing, intracellular staining for viral nucleoprotein (NP)-1, was
86 performed using BD Cytotfix/Cytoperm kit according to manufacturer's instructions,
87 and AlexaFluor 488 (AF488)-conjugated anti-NP1 antibody (HB-65, a kind gift of
88 3VBiosciences). The gating strategy is shown in Figure 1A.

89 MDMs & blood T cells:

90 Isolated macrophages were incubated on ice in the dark for 30 min with the following
91 antibodies: PE-conjugated anti-PD-L1, Allophycocyanin (BD Biosciences or
92 appropriate isotype controls. After washing, intracellular staining for viral
93 nucleoprotein (NP)-1, was performed using BD Cytotfix/Cytoperm kit according to
94 manufacturer's instructions, and AlexaFluor 488 (AF488)-conjugated anti-NP1
95 antibody (HB-65, a kind gift of 3VBiosciences).

96 Flow cytometric analysis was performed on a FACSAria using FACSDiva
97 software v5.0.3 (all BD).

98

99 **ELISpot**

100 Monocyte-depleted PBMC were defrosted at room temperature and suspended in
101 RS RPMI. MDMs were removed from 24-well culture plate using non-enzymatic cell
102 dissociation solution (Sigma) and transferred to sterile 1.5 ml Eppendorf tubes. Cells
103 were centrifuged at 400 g, 4°C, 5 min before resuspension in serum-free (SF) RPMI
104 containing L-glutamine, penicillin/streptomycin, and fungizone. MDMs were either
105 not infected, or were treated with 2.5×10^4 pfu/ml X31 Influenza A H3N2 virus at
106 37°C for 2 h before washing and resuspending in RS RPMI.

107 ELISpot for Human IFN- γ was then performed using 0.45 μ m MultiScreen-IP
108 Filter Plates (Millipore, Watford, UK) following manufacturer's instructions (MabTech,

109 Stockholm, Sweden). Briefly, coating antibody (1-D1K) was diluted to 15 µg/ml in
110 sterile DPBS and was added to the plate before overnight incubation at 4°C. Plates
111 were then washed five times with sterile DPBS before replacement with SF RPMI for
112 30 min at RT. The SF-media was then removed and MDM were added to each well
113 at a concentration of 5×10^4 cells/well and 2.5×10^5 monocyte-depleted PBMC or $1 \times$
114 10^5 CD8+ T cells were added to MDM-containing wells and incubated at 37°C. After
115 22 h, the plate was washed five times with sterile DPBS + 0.05% Tween20 (Sigma).
116 Detection antibody (7-B6-biotin) was diluted to 1 µg/ml in sterile DPBS + 0.5% FBS
117 and was added to the plate which was then incubated at RT. After 2 h, the plate was
118 washed five times with sterile DPBS before addition of Streptavidin-ALP (diluted
119 1:1000 in sterile DPBS+0.5% FCS) and incubation for 1 h at RT. Plates were then
120 washed with sterile DPBS before replacement with substrate solution (BCIP/NBT
121 diluted 1:1:8 in sterile H₂O). Plate was incubated at RT for 2-5m until clear spots
122 were visible. At this point wells were washed five times with dH₂O and allowed to dry
123 at RT. Spot development was analysed using an AID EliSpot Reader (Germany) and
124 AID EliSpot Software (Germany).

125 In initial experiments, no IFN γ staining was seen in wells containing infected
126 MDM or lymphocytes alone (1). Peripheral blood T cells do not appear to be
127 infected when exposed to X31 (1).

128

129 **RNA Isolation & RT-PCR**

130 RNA was extracted from T cells using a Stratagene Microprep Kit (Agilent
131 Technologies, Stockport, UK). Reverse transcription was carried out using a High
132 Capacity cDNA Reverse Transcription Kit (Life Technologies) with random hexamers
133 carried out according to the manufacturer's protocols. *TIM3* gene expression was

134 analysed using TaqMan universal PCR master mix, No AmpErase® UNG in a
135 7900HT fast real-time PCR system machine (all Life Technologies). Gene
136 expression was normalized to β_2 -microglobulin gene expression and quantified using
137 the $\Delta\Delta C_T$ method.

138

139 **Supernatant analyses**

140 IFN β concentrations in culture supernatants were measured by ELISA according to
141 the manufacturer's instructions (MSD, Gaithersberg, USA). Culture supernatants
142 were analysed by Luminex assay for IFN γ as per manufacturer's instructions (Bio-
143 Rad, Hemel Hempstead, UK).

144

145 **Statistics**

146 Analysis of two groups was performed using Wilcoxon's signed rank test for paired
147 data and a Mann-Whitney U test for unpaired data. Chi-squared test and Fishers
148 exact test were used for categorical data (GraphPad Prism v6, GraphPad Software
149 Inc., San Diego, USA). Results were considered significant if $p < 0.05$.

150

151 **Results**

152

	Control	COPD	p Value
N	20	24	-
Age (years)	68 (60.25 – 74.75)	67 (59.75 - 74)	0.89#
Gender M/F	9 / 11	12 / 12	0.741†
BMI	28 (24.55 – 32.1)	23.85 (21.45 – 27.7)	0.08#
Confirmed corticosteroid use	1	7	0.0544‡
Smoker (Never/Ex/Current)	5 / 11 / 4	1 / 16 / 7	0.13‡
Pack Years	20 (0.9 – 55.25)	40 (29 – 56.25)	0.11#
FEV ₁ %	95 (85.45 – 112.2)	76.1 (64.56 – 88.88)	< 0.001#
FEV ₁ /FVC ratio	0.752 (0.727 – 0.8074)	0.612 (0.524 – 0.668)	< 0.0001#

153 Supplementary Table 1: Clinical characteristics of surgical patients shown in Figure 1
 154 B+C. Data are presented as median and IQR shown. Ex-smokers were defined as
 155 individuals who had stopped smoking for > 6 months prior to surgery. BMI data
 156 shown represents 13 Control and 16 COPD patients. #Mann Whitney U Test, †Chi-
 157 squared test, ‡ Fishers Exact test
 158
 159

	Control	COPD	p Value
N	10	14	-
Age (years)	70.5 (58.75 – 76.5)	67 (61.25 – 72.25)	0.627#
Gender M/F	4 / 6	6 / 8	1.00†
BMI	22.4 (21.7 – 28.9)	28.3 (22.6 – 36.4)	0.9#
Confirmed corticosteroid use	1	4	0.3577‡
Smoker (Never/Ex/Current)	2 / 7 / 1	0 / 8 / 6	0.065#
Pack Years	40 (1.5 – 56)	40 (34.38 – 66.25)	0.35#
FEV ₁ %	98 (93 – 114)	73 (62 – 78.5)	< 0.001#
FEV ₁ /FVC ratio	0.747 (0.747 – 0.797)	0.605 (0.523 – 0.642)	< 0.0001#

160 Supplementary Table 2: Clinical characteristics of surgical patients shown in Figures
 161 2-5. Data are presented as Median and IQR shown. Ex-smokers were defined as
 162 individuals who had stopped smoking for > 6 months prior to surgery. BMI data
 163 shown represents 3 Control and 5 COPD patients. #Mann Whitney U Test, †Chi-
 164 squared test, ‡ Fishers Exact test
 165

Control (24)	COPD (33)
24 Lung cancer	33 Lung cancer
2 Hypertension	5 Hypertension
2 Hypercholesterolaemia	4 Hypercholesterolaemia
2 Arthritis	4 Arthritis
1 Hypothyroidism	3 Hypothyroidism
2 Hysterectomy	3 Hysterectomy
1 Hip replacement	2 Hip replacement
2 Appendectomy	1 Appendectomy
1 Abdominal aortic aneurysm	1 Abdominal aortic aneurysm
1 Varicose veins	1 Varicose veins
1 Irritable Bowel Syndrome	1 Irritable Bowel Syndrome
1 Throat polyps	1 Throat polyps
1 Skin cancer	1 Skin cancer
2 Type 2 Diabetes	1 Type 1 Diabetes

166 Supplementary Table 3: Common comorbidities of surgical patients. Number
 167 indicates incidence in each group. Numbers do not sum as each patient can have
 168 more than one co-morbidity.
 169

170 **Supplementary Figure Legends**

171

172 **Supplementary Figure E1. CD4+ and CD8+ T cell population in human lung**

173 **parenchymal tissue**, Unstained singlet population was obtained from digested

174 tissue. Dead cells were excluded using LIVE/DEAD® Fixable Aqua Dead Cell Stain.

175 Live singlet CD45+ population was then identified and from this a CD45+CD3+ T cell

176 population. The CD45+CD3+ T cell population was divided into CD4+ and CD8+ T

177 cells. **(A)** Control samples **(B)** and COPD samples displaying their paired T cell

178 populations. Control n = 20, COPD n = 24.

179

180 **Supplementary Figure E2. Flow cytometry gating strategy for memory CD4+**

181 **and CD8+ T cells. Naïve and Tmem cell populations in blood and tissue.**

182 PBMCs were isolated from blood using Ficoll-Paque density centrifugation. Tissue

183 was prepared as previously described and digested in 0.5 mg/ml collagenase

184 solution for 15 min. **(A+C)** T cell populations were gated on a singlet

185 CD3+CD4+CD8- population or **(B+D)** a singlet CD3+CD4-CD8+ population. **(A)**

186 CD4+ memory populations and **(B)** CD8+ populations in blood. **(C)** CD4+ memory

187 populations and **(D)** CD8+ populations in lung parenchymal tissue. Flow cytometry

188 dot plots representative of at least 5 independent experiments.

189

190 **Supplementary Figure E3. RT-PCR gene expression of TIM-3 by T cells isolated**

191 **from lung tissue.** T cells were gated on the live CD45+CD3+ population. **(A)** RT-

192 PCR was performed with 2.5×10^4 CD4+ **(B)** or CD8+ T cells sorted from control or

193 COPD lung parenchyma. $\Delta\Delta C_t$ value calculated using B2M housekeeping gene

194 expression. n = 6

195

196 **Supplementary Figure E4. Proportion of CD4+ and CD8+ T cells which express**
197 **PD-1 in response to tissue infection by X31 influenza. (A)** Proportion of CD4+ **(B)**
198 and CD8+ T cells which expressed PD-1 was quantified by flow cytometry in non-
199 infected (NI), live X31 virus infection (X31) and UV-irradiated virus (UVX31) lung
200 samples. **(C)** The fold increase in PD-1 expression (sMFI) of CD4+ **(D)** and CD8+ T
201 cells between NI and X31-infected samples and NI and UVX31 (UV)- treated
202 samples from COPD patients (n=12). **(E)** The fold increase in PD-1 expression
203 (sMFI) of CD4+ **(F)** and CD8+ T cells between NI and X31 samples was also
204 calculated for Control samples (n = 9) and COPD samples (n = 12). Median and IQR
205 shown, Data analysed using a Wilcoxon-signed rank test * p<0.05, ** p<0.01.

206

207 **Supplementary Figure E5. PD-L1 expression by epithelial cells during X31**
208 **infection of lung parenchyma.** 1cm³ sections of tissue were treated with UVX31,
209 X31 or NI for 2 h before a 22 h incubation. Proportions of epithelial cells expressing
210 PD-1 was quantified by flow cytometry. Control n = 9, COPD n = 11. Median and
211 IQR shown.

212

213

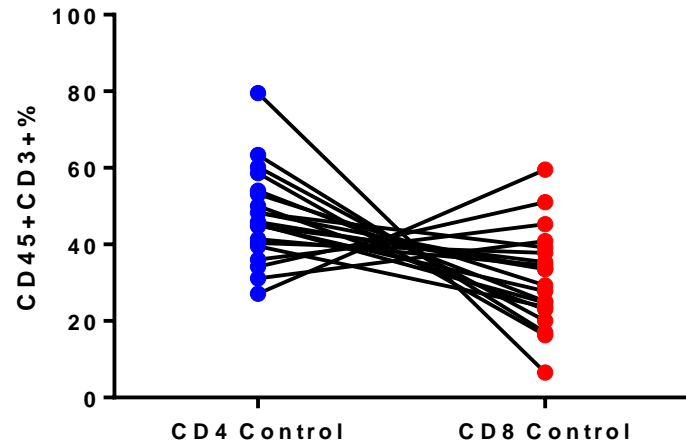
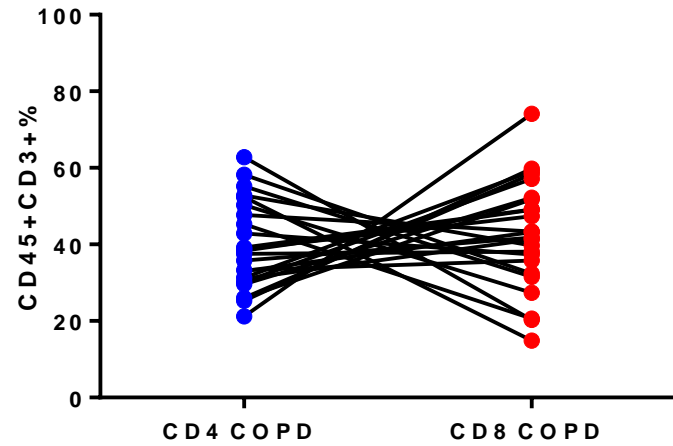
214 **References**

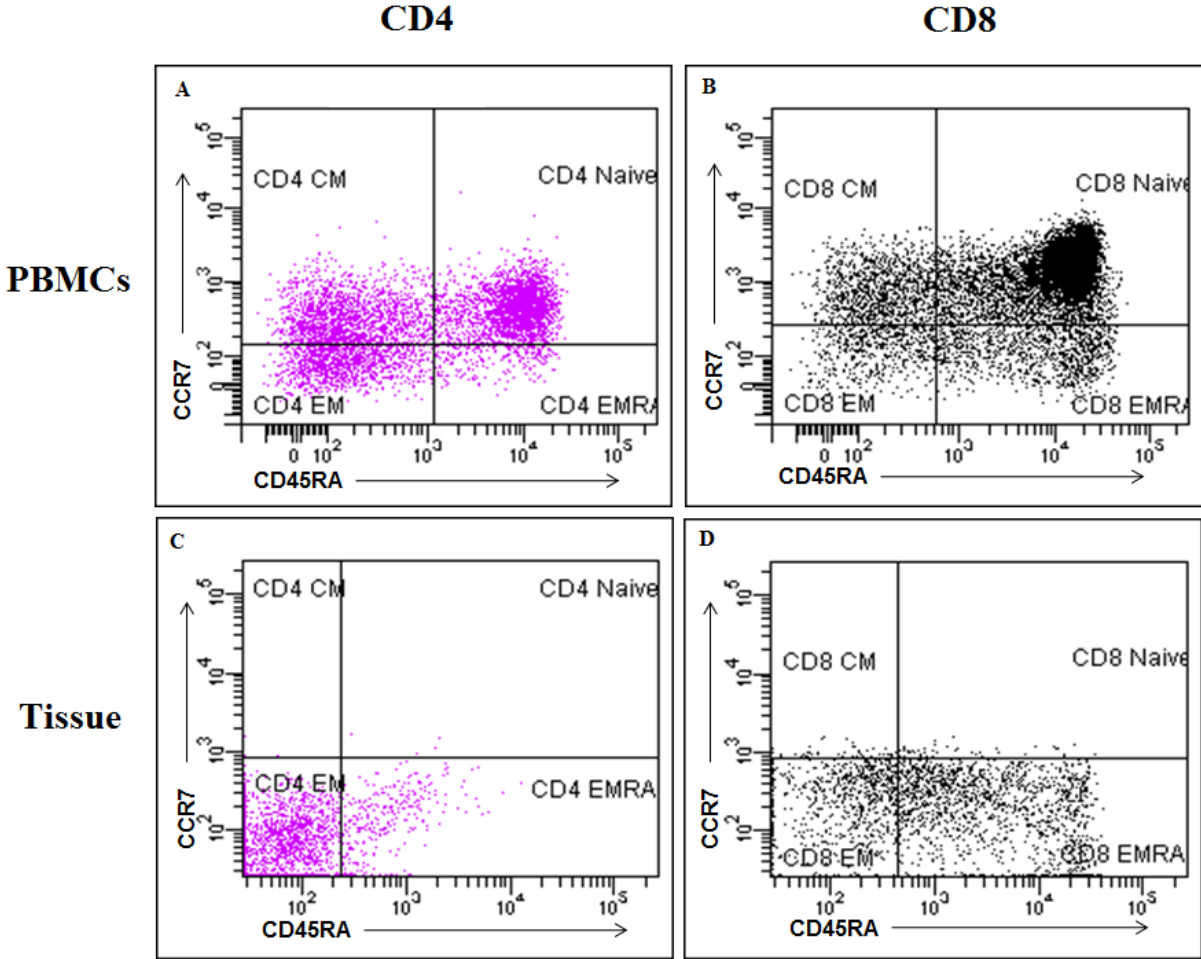
215 1. Staples KJ, Nicholas B, McKendry RT, Spalluto CM, Wallington JC, Bragg
216 CW, Robinson EC, Martin K, Djukanovic R, Wilkinson TM. Viral infection of human
217 lung macrophages increases pdl1 expression via ifnbeta. *PLoS One*
218 2015;10:e0121527.

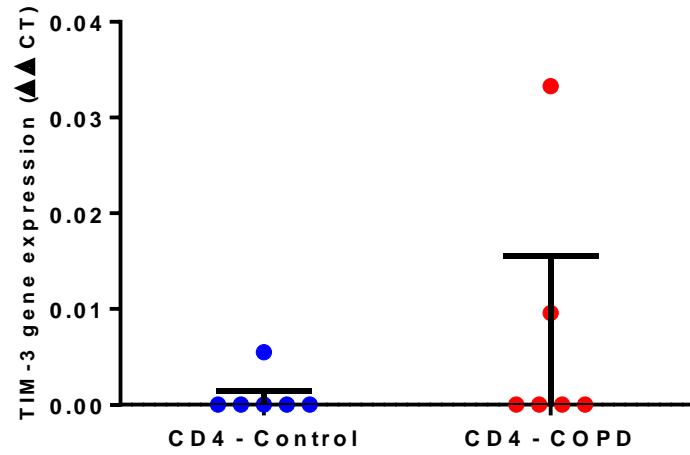
219
220 2. Holt PG, Robinson BW, Reid M, Kees UR, Warton A, Dawson VH, Rose A,
221 Schon-Hegrad M, Papadimitriou JM. Extraction of immune and inflammatory cells
222 from human lung parenchyma: Evaluation of an enzymatic digestion procedure. *Clin*
223 *Exp Immunol* 1986;66:188-200.

224

225

A**B**



A**B**